
The multi-orbits skew spectrum: boosting permutation-invariant data representations

Anonymous Author(s)

Anonymous Affiliation

Anonymous Email

Abstract

1
2 We generalize the concept of skew spectrum of a graph, a group-theoretical
3 permutation-invariant feature mapping. The skew-spectrum considers adjacency
4 matrices as functions over \mathbb{S}_n and leverages Fourier transform and group-theoretical
5 tools to extract features that are invariant under the group action. The main short-
6 coming of the previous result is that the skew spectrum only works for unlabeled
7 graphs. The reason is that these graphs can be represented using matrices whose
8 main diagonal contains zeros, meaning that there is only one set of elements that
9 can permute among themselves (i.e., one orbit). However, the representations of
10 more complex graphs (e.g., labeled graphs, multigraphs, or hypergraphs) have
11 different sets of elements that can consistently permute on different orbits. In this
12 work, we generalize the skew-spectrum to the multiple orbits case. Our multi-
13 orbits skew spectrum produces features invariant to such permutations and possibly
14 informative of non-consistent ones. We believe this method can improve the per-
15 formances of models that learn on graphs. Moreover, the theory is general enough
16 to handle invariance under the action of any finite group on multiple orbits and has
17 applications beyond the graph domain.

18 1 Introduction

19 In the past decade, machine learning on datasets representing data as tensors became an active area
20 of research. This trend is fueled by important applications in anomaly detection, medical imaging,
21 genomics, and many others [1–3]. We generalize the skew spectrum, a graph invariant proposed
22 in [4], to a new tensor invariant. In the context of graphs, for which we frame this manuscript,
23 our generalization extends the applicability of this feature extraction method to more complex data
24 structures, such as labelled graphs, multigraphs, and hypergraphs.

25 The skew spectrum of a graph is a permutation invariant mapping from the adjacency matrix $A \in$
26 $\mathbb{R}^{n \times n}$ of a weighted, directed, *unlabeled* graph \mathcal{G} to a new feature space. A graph is unweighted when
27 the entries of A are just elements of $\{0, 1\}$, undirected when $A^T = A$, and unlabeled when $A_{ii} = 0$
28 for $i \in [n]$. This mapping interprets the graph as a function on the symmetric group $f : \mathbb{S}_n \mapsto \mathbb{R}$,
29 where n is the number of nodes in the graph. The function f is defined as $f(\sigma) = A_{\sigma(n), \sigma(n-1)}$, for
30 $\sigma \in \mathbb{S}_n$, here $\sigma \in \mathbb{S}_n$ is permutation of the set $[n]$ and $\sigma(n)$ is the image of n under the permutation
31 σ . For more precise definitions on graph theory we refer the reader to Appendix A. Leveraging
32 techniques from non-commutative harmonic analysis it is possible to see that the skew spectrum
33 of a function f is related to the Fourier transform of the triple correlation of f [5]. An entry of the
34 skew spectrum is a matrix, which we denote as $\mathcal{S}(f; \sigma, \rho)$, which is a function of a permutation
35 $\sigma \in \mathbb{S}_n$, and an irreducible representation ρ . We recall that a representation of \mathbb{S}_n is a map ρ from
36 the group \mathbb{S}_n to a subgroup of the orthogonal group on a real, finite-dimensional vector space. The
37 representation ρ is irreducible if it cannot be decomposed into direct sum of other representations.
38 The intuition here is that $\mathcal{S}(f; \sigma, \rho)$ is a polynomial of third order in the adjacency matrix such that
39 this polynomial is invariant with respect to joint permutations of rows and columns of the adjacency
40 matrix. While the skew spectrum might be a *complete* invariant in some cases [6], this is not true
41 for many many applications of the skew spectrum to permutation-invariant representations (i.e., two
42 non-isomorphic graphs could be mapped to the same feature vector).

43 The reduced skew spectrum [4, Definition 2] is a lightweight version of the skew spectrum, which
 44 is defined by reducing the size of the matrices of $\mathcal{S}(f; \sigma, \rho)$. The motivation for using the reduced
 45 skew spectrum is threefold: While the computation of the skew spectrum has a complexity of $O(n^6)$,
 46 the reduced skew spectrum has a computational complexity of $O(n^3)$ only (here n is the number of
 47 the nodes of the graph); the output size of the reduced skew spectrum is independent of n and skew
 48 spectrum contains many entries which are trivially zero, the reduced skew spectrum eliminates almost
 49 all such entries. The (reduced) skew spectrum can only be applied to datasets with a single orbit; this
 50 limitation is particularly important when dealing with tensor datasets. In this work, we extend the
 51 skew spectrum to the multi-orbits setting. We show how we can inherit good computational properties
 52 of the reduced skew spectrum also for the multiple orbit setting. While the main contribution of
 53 this work is theoretical, we corroborate our analysis with some prototypical experiments on real and
 54 synthetic datasets. We conclude that the multiple-orbits skew spectrum can enhance the representation
 55 of datasets where keeping a consistency between permutation on different orbits is important.

56 2 The multi-orbits skew spectrum

57 The main idea in generalizing the skew spectrum to multiple orbits is two-fold: we replace the
 58 function $f : \mathbb{S}_n \mapsto \mathbb{R}$ by a vector-valued function $f : \mathbb{S}_n \mapsto \mathbb{R}^k$, where k is the number of orbits, and
 59 we replace products of functions by tensor products. For simplicity, we will describe the computation
 60 for the case of two orbits for a function generated by the adjacency matrix $A \in \mathbb{R}^{n \times n}$ of a graph \mathcal{G} .
 61 Note, however, that all of our formulas are valid for any finite number of orbits. The interested reader
 62 can refer to Appendix A for the representing more complex graphs as functions.

63 A labeled graph is one for which the adjacency matrix has some non-zero entries on the diagonal.
 64 For a given labeled graph \mathcal{G} , the adjacency matrix A is unique only up to arbitrary permutations of
 65 the same indexes of both rows and columns. If we can obtain the adjacency matrix of a graph \mathcal{G} by
 66 applying a permutation $\sigma \in \mathbb{S}_n$ to the indexes of the adjacency matrix of another graph $\tilde{\mathcal{G}}$, then we
 67 say the graphs are isomorphic. It is fairly easy to see that the adjacency matrix of a labeled graph has
 68 two orbits: the main diagonal, and the off-diagonal. For $\sigma \in \mathbb{S}_n$, let $f : \mathbb{S}_n \mapsto \mathbb{R}^2$ be defined as

$$f(\sigma) = \begin{pmatrix} A_{\sigma(n), \sigma(n)} \\ A_{\sigma(n), \sigma(n-1)} \end{pmatrix}. \quad (1)$$

69 We define an entry of the multi-orbits skew spectrum as

$$\mathcal{S}(f; \sigma, \rho) = \frac{1}{(n!)^2} \sum_{\tilde{\sigma}_1 \in \mathbb{S}_n} \sum_{\tilde{\sigma}_2 \in \mathbb{S}_n} f(\tilde{\sigma}_1) \otimes f(\tilde{\sigma}_1 \sigma) \otimes f(\tilde{\sigma}_2) \otimes (\rho(\tilde{\sigma}_1)^\dagger \rho(\tilde{\sigma}_2)), \quad (2)$$

70 where \dagger denotes the usual complex conjugate transpose. From this formula, one can notice that
 71 the skew spectrum entries are invariant to permutations of the indices of the adjacency matrix, see
 72 Appendix B for a formal proof and some intuition on the invariance.

73 Naively computing one skew spectrum entry from Eq. 2 would require $O((n!)^2)$ steps, which soon
 74 becomes computationally infeasible even for small graphs. However, we can significantly speed
 75 up the calculation using insights from group theory. Up to improvements of constant factors, our
 76 computational speedups coincide with the ones presented in Kondor and Borgwardt [4] and so the
 77 computational cost is $O(n^6)$ (we are considering $k = 2$ as a constant). The key insight on the
 78 computational optimization that we adapt from the single-orbit case is the following. Denoting \hat{f} the
 79 Fourier transform of f and writing

$$\hat{f}(\rho) = \frac{1}{n!} \sum_{\tilde{\sigma} \in \mathbb{S}_n} f(\tilde{\sigma}) \otimes \rho(\tilde{\sigma}) \quad \text{and} \quad \hat{r}_f(\sigma, \rho) = \frac{1}{n!} \sum_{\tilde{\sigma} \in \mathbb{S}_n} f(\tilde{\sigma}) \otimes f(\tilde{\sigma} \sigma) \otimes \rho(\tilde{\sigma}) \quad (3)$$

80 we get that Equation 2 can be rewritten as $\mathcal{S}(f; \sigma, \rho) = \hat{r}_f^\dagger(\sigma, \rho) \odot \hat{f}(\rho)$, where \odot denotes tensor
 81 product of functions and matrix product of representations. This significantly speeds up the calculation
 82 since the calculation of \hat{f} can be reduced to sum only over $n(n-1)$ elements (as a property of f)
 83 and the calculation of \hat{r}_f can be reduced in a similar way, via Clausen-FFT type of arguments [5, 7].

84 At the same time, Kondor and Borgwardt [4] show that the skew spectrum needs to be computed for
 85 only 7 group entries and 4 irreducible representations, fixing the overall computation of the skew

86 spectrum to $O(n^6)$. It is possible to prove that we actually need only 6 group elements. Indeed, 2 of
 87 the 7 are one the inverse of each other and having both of them does not introduce extra information.
 88 Moreover, we have empirical evidence that one of the 4 irreducible representation only produces 0
 89 matrices for undirected graphs and can therefore be discarded in such case, though we do not have a
 90 formal proof of this yet.

91 While the computational complexity is polynomial in the size of the graph, there are still two problems:
 92 $O(n^6)$ starts to be infeasible for medium-sized graphs and the number of computed features scales
 93 with the number of nodes. Both of these problems are solved by using the reduced skew spectrum [4].
 94 The main idea is that the Fourier transform \hat{f} consists of matrices that have variable number of rows
 95 but fixed number of columns, so the variable size of skew spectrum comes only from \hat{r}_f . We thus
 96 compute the reduced skew spectrum by limiting the number of rows of \hat{r}_f , producing matrices of
 97 fixed size for all n , with a computational complexity of $O(n^3)$. In the general case with k orbits the
 98 computational complexity of the reduces skew spectrum becomes $O(k^2n^3 + k^3n^2)$. For a symmetric
 99 adjacency matrix of a graph with n nodes, the single-orbit reduced skew spectrum consists of 36
 100 numbers, while the two-orbits reduced skew spectrum consists of 288 numbers. In general, for k
 101 orbits, the reduced multi-orbits skew spectrum consists of $36k^3$ numbers.

102 **Generalization to multigraphs and hypergraphs.** We present the generalization of our method to
 103 multigraphs. Different types of edges can be seen as several adjacency matrices and we can treat those
 104 as additional orbits. Consider a multigraph with two types of edges. Let A be the adjacency matrix
 105 corresponding to the first type of edges and let B be adjacency matrix corresponding to the second
 106 type of edges (note that the diagonals of both A and B coincide since the labels of the nodes are always
 107 the same). We can then construct the function $f_{AB}(\sigma) = (A_{\sigma(n),\sigma(n)}, A_{\sigma(n),\sigma(n-1)}, B_{\sigma(n),\sigma(n-1)})^\top$
 108 and use the skew spectrum (or reduced skew spectrum) of f_{AB} .

109 We can always represent a hypergraph as a multigraph where each edge type is an edge, but we also
 110 propose an alternative encoding. Consider first hyperedges that connect exactly 3 nodes. We can
 111 then represent these hyperedges via $n \times n \times n$ adjacency tensor A such that A_{abc} , $a \neq b \neq c \neq a$, is
 112 the weight of the hyperedge connecting the nodes labeled by a , b , and c . We can then use similar
 113 methods to construct the corresponding function f and compute its skew spectrum. We can use similar
 114 approach for hypergraphs with hyperedges connecting at most k nodes by considering adjacency
 115 tensors $A_{a_1 \dots a_k}$. With this alternative representation, and still considering the amount of orbits as a
 116 constant, the computational complexity of the skew spectrum and the reduced skew spectrum will
 117 increase. This is because for a standard graph the computational speedup heavily relies on the fact
 118 that the function f is S_{n-2} symmetric, but, for example, for hypergraph with hyperedges connecting
 119 at most 3 nodes the resulting function will be only S_{n-3} symmetric. Thus, for example, one would
 120 need to sum at least $n(n-1)(n-2)$ elements in order to compute $\hat{f}(\rho)$.

121 3 Numerical Experiments

122 We implemented the code for both the single-orbit skew spectrum and the multi-orbits skew spectrum.
 123 In this section, we report some prototypical experiments using their reduced versions on labeled
 124 graphs. The experiments aim to show the enhanced representation power of the multi-orbits skew
 125 spectrum against its predecessor. Comparison with other state-of-the-art graph invariants is out
 126 of the scope of this manuscript and is left for future work. We discuss some extra experiments in
 127 Appendix C.

128 3.1 Graph classification on a synthetic dataset

129 The dataset contains undirected, unweighted, and labeled graphs. The node labels assume all the
 130 values between 0 and $n-1$, with n the number of nodes. The labels are encoded along the main
 131 diagonal of the graphs' adjacency matrices. The dataset consists of four families of graphs, namely
 132 15A, 15B, 6A, and 6B (Fig. 1 illustrates one graph representative per family). Each family contains
 133 1000 isomorphic graphs, meaning that, inside a family, all the graphs are equal up to permutations that
 134 are simultaneously edge-preserving and label-preserving. The graphs in 15A and 15B are equivalent
 135 up to edge-preserving permutations but are not isomorphic if we also consider the labels permutations,
 136 and so are the graphs in 6A and 6B. The task is to classify the four families of graphs correctly.

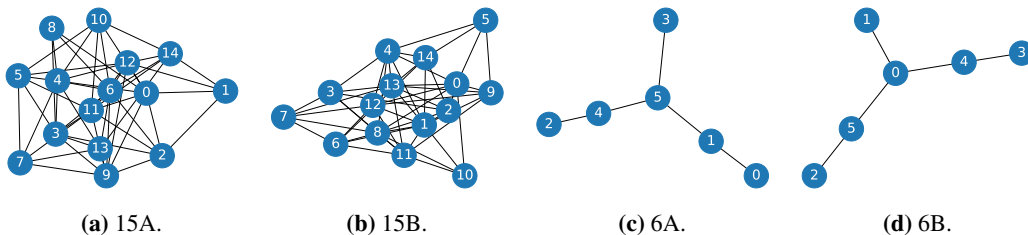


Figure 1: Synthetic dataset’s graph families representatives.

137 We have processed this dataset twice, producing two different representations. The first one consists
 138 of a concatenation of the outputs of the single-orbit skew spectrum computed separately on the
 139 off-diagonal and on the main diagonal elements of the adjacency matrix (i.e., each skew spectrum
 140 uses one row of Eq. 1 as a function). The second one consists of the output of the two-orbits skew
 141 spectrum (computed using Eq. 1). We trained a random forest (60 estimators, no max depth) on the
 142 two representations, holding out a balanced 20% of the dataset for testing purposes. The classifier
 143 achieves an accuracy of 0.5 on the single-orbit representation and of 1 on the 2-orbits one, meeting
 144 our expectations. This is because the concatenation of single-orbit skew spectra cannot distinguish
 145 the couples 15A-15B and 6A-6B, whose labels and edges are linked by different permutations.

146 3.2 Atomization energy regression on QM7

147 The dataset is composed of a list of 23×23 matrices representing the Coulomb matrices of 7165
 148 molecules composed of up to 23 atoms, from which up to 7 are considered heavy atoms [8, 9]. The
 149 Coulomb matrix $C \in \mathbb{R}^{23 \times 23}$ is defined as $C_{ii} = \frac{1}{2} Z_i^{2.4}$ and $C_{ij} = \frac{Z_i Z_j}{|R_i - R_j|}$, where Z_i is the nuclear
 150 charge of the i -th atom of the molecule, and R_i is its position. The learning task associated with this
 151 dataset is to predict the atomization energies of the molecules (kcal/mol), which are reals in the range
 152 $[-2000, -800]$ renormalized in $[-1, 1]$. We compute the reduced single-orbit skew spectrum on the
 153 off-diagonal elements and the multiple-orbits skew spectrum and use them for regression, holding
 154 out 20% of the dataset for the test set. Table 1 summarizes the results.

Table 1: Regression on qm7 with different features. We tested the following machine learning models: Extreme Gradient Boosting (Xgboost), Gradient Boosting Regressor (GBR), Elastic Net (EN), Linear Regression (Linear) using the default parameters of sk-learn[10]. Linear regression cannot fit the dataset for the eigenvectors of the Coulomb matrix. The error is measured as Mean Absolute Error.

Representation	Xgboost	GBR	EN	Linear
Single-orbit	29.15	36.55	114.68	61.15
2-orbits	18.28	27.12	58.60	49.45
CM’s eigs	38.047	37.92	47.83	-
Laplacian’s eigs	23.52	26.93	47.62	47.80

155 Using the multi-orbits skew spectrum we improve the models using the single-orbit skew-spectrum.

156 4 Conclusions

157 This work presents a generalization of the skew spectrum to multiple orbits. Thanks to our implemen-
 158 tation, we can test the performances of the multi-orbits skew spectrum on classification and regression
 159 tasks. The performances obtained in these prototypical experiments highlight the limitations of
 160 the single-orbit skew spectrum and the advantages of the proposed solution. For the classification
 161 experiment, we have a clear separation between the performances of a simple learner on 1-orbit and
 162 2-orbits skew spectra of labeled graphs. For regression, the 2-orbits skew spectrum can improve the
 163 mean absolute error compared to the single orbit case of all the machine learning models studied. We
 164 leave for future work the study of problems on tensor datasets where the multi-orbits skew spectrum
 165 can outperform state-of-the-art machine learning models.

References

- 166
- 167 [1] Yh Taguchi and Turki Turki. Novel feature selection method via kernel tensor decomposition
168 for improved multi-omics data analysis. *BMC medical genomics*, 15(1):1–12, 2022. 1
- 169 [2] Hadi Fanaee-T and João Gama. Tensor-based anomaly detection: An interdisciplinary survey.
170 *Knowledge-Based Systems*, 98:130–147, 2016.
- 171 [3] Derek K Jones, Lewis D Griffin, Daniel C Alexander, Marco Catani, Mark A Horsfield, Robert
172 Howard, and Steve CR Williams. Spatial normalization and averaging of diffusion tensor mri
173 data sets. *Neuroimage*, 17(2):592–617, 2002. 1
- 174 [4] Risi Kondor and Karsten M Borgwardt. The skew spectrum of graphs. In *Proceedings of the*
175 *25th international conference on Machine learning*, pages 496–503, 2008. 1, 2, 3
- 176 [5] Risi Kondor. The skew spectrum of functions on finite groups and their homogeneous spaces.
177 *arXiv preprint arXiv:0712.4259*, 2007. 1, 2
- 178 [6] Ramakrishna Kakarala. *Triple correlation on groups*. University of California, Irvine, 1992. 1
- 179 [7] Michael Clausen. Fast generalized fourier transforms. *Theoretical Computer Science*, 67(1):
180 55–63, 1989. 2
- 181 [8] M. Rupp, A. Tkatchenko, K.-R. Müller, and O. A. von Lilienfeld. Fast and accurate modeling
182 of molecular atomization energies with machine learning. *Physical Review Letters*, 108:058301,
183 2012. 4
- 184 [9] L. C. Blum and J.-L. Reymond. 970 million druglike small molecules for virtual screening in
185 the chemical universe database GDB-13. *J. Am. Chem. Soc.*, 131:8732, 2009. 4
- 186 [10] F. Pedregosa, G. Varoquaux, A. Gramfort, V. Michel, B. Thirion, O. Grisel, M. Blondel,
187 P. Prettenhofer, R. Weiss, V. Dubourg, J. Vanderplas, A. Passos, D. Cournapeau, M. Brucher,
188 M. Perrot, and E. Duchesnay. Scikit-learn: Machine learning in Python. *Journal of Machine*
189 *Learning Research*, 12:2825–2830, 2011. 4

190 A Representing graph data using functions

191 In this section we describe some categories of graphs and how we can represent them using functions
 192 of the form $f : \mathbb{S}_n \mapsto \mathbb{R}^k$. Rather than being an exhaustive list, this section should give the reader an
 193 idea of how to construct functions for more complex data structures.

194 The simplest class of graphs that we can represent are directed, weighted graphs with n nodes. Such
 195 graphs can be represented using an adjacency matrix $A \in \mathbb{R}^{n \times n}$ with entries equal to 0 on the main
 196 diagonal. In this case, we can build a function $f : \mathbb{S}_n \mapsto \mathbb{R}$, as

$$f(\sigma) = A_{\sigma(n), \sigma(n-1)}, \quad (4)$$

197 where $\sigma(i)$ denotes the image of n under the permutation σ . The function takes a permutation as
 198 input and outputs a matrix element, using the image of n and $n - 1$ under this permutation (it only
 199 iterates over the non-diagonal elements of A). This is the function of the original skew spectrum.
 200 Plugging this function in our multi-orbit skew spectrum formulation will give the same result as the
 201 single-orbit skew spectrum.

202 Generalizing to some more complex graph structures, we consider graphs whose nodes can be
 203 associated with one attribute.

204 **Definition 1** (Labeled graph). *Labeled graphs are graphs whose nodes have one attribute that can*
 205 *be encoded as a real number.*

206 We can represent such graphs using the same adjacency matrix $A \in \mathbb{R}^{n \times n}$, and we could encode the
 207 attribute of the node i in the diagonal entry A_{ii} . In this case, we want to be sure that a permutation
 208 will consistently move both the edges and the node labels. Those live in two different orbits, that
 209 need to permute accordingly. In this case, we can construct the graph function $f : \mathbb{S}_n \mathbb{R}^2$ as

$$f(\sigma) = \begin{bmatrix} A_{\sigma(n), \sigma(n-1)} \\ A_{\sigma(n), \sigma(n)} \end{bmatrix}. \quad (5)$$

210 Here the order of the elements in the output vector in \mathbb{R}^n does not matter, as long as the choice is
 211 consistent during the computation. Given a permutation σ , this function returns a vector containing
 212 an element on the off-diagonal and an element on the diagonal of A .

213 A more general class of graphs are graphs with node attributes.

214 **Definition 2** (Graph with node attributes). *A graph with node attributes is a graph whose nodes are*
 215 *associated to a vector of attributes, represented by real numbers.*

216 Say that each node can contain at most k' distinct attributes. Then, we can represent the graph using
 217 an adjacency matrix $A \in \mathbb{R}^{n \times n}$ with zeroes on the main diagonal and a set of k' vectors $x_i \in \mathbb{R}^n$
 218 for $i \in \{0, \dots, n-1\}$. Each vector x_i represents an attribute and contains n entries, one per node.
 219 In this case, off-diagonal elements of A can permute among themselves, entries in the same x_i can
 220 permute among themselves, but they have to do so consistently, forming $k = k' + 1$ orbits. We
 221 represent the j^{th} entry of x_i as $x_{i,j}$ and it represents the value of the attribute i for the node j . We
 222 can construct the relative graph function $f : \mathbb{S}_n \mapsto \mathbb{R}^{k'+1}$ as

$$f(\sigma) = \begin{bmatrix} A_{\sigma(n), \sigma(n-1)} \\ x_{1, \sigma(n)} \\ x_{2, \sigma(n)} \\ \dots \\ x_{k', \sigma(n)} \end{bmatrix}. \quad (6)$$

223 Even in this case, the matrix outputs one element per orbit.

224 Going on with more complex data structures, we can show how to represent multigraphs.

225 **Definition 3** (Multigraph). *Multigraphs are are graphs where an edge can connect the multiple*
 226 *nodes.*

227 Say that we have k different layers of edges, each layer having its own meaning. Then, we can
 228 represent the graph using a tensor adjacency matrix $A \in \mathbb{R}^{k \times n \times n}$, where $A_{k,i,j}$ represents the value
 229 of the edge in layer k between nodes i and j . The k layers form k distinct orbits where permutations
 230 need to occur consistently. We can construct the graph function $f : \mathbb{S}_n \mapsto \mathbb{R}^k$ as

$$f(\sigma) = \begin{bmatrix} A_{0, \sigma(n), \sigma(n-1)} \\ A_{1, \sigma(n), \sigma(n-1)} \\ \dots \\ A_{k-1, \sigma(n), \sigma(n-1)} \end{bmatrix}. \quad (7)$$

231 Whenever we wanted to consider multigraphs with node attributes, we could increment the number
 232 of orbits and build bigger functions.

233 About hypegraphs, we refer the reader to the intuition in the main text. We recall that the computation
 234 easily starts to become unpractical for hypergraphs having edges connecting more than a handful of
 235 nodes (say 6). This is because the formulation for hypergraphs introduces a dependency on m in the
 236 runtime (rather than k), which is provably at least factorial $m!$.

237 B Invariance of the multi-orbit skew spectrum

238 **Definition 4** (Multi-orbit skew spectrum).

239 **Theorem 5.** *Let $f_1(\sigma) : \mathbb{S}_n \mapsto \mathbb{R}^k$ be a function that maps an element of the permutation group to*
 240 *a vector of real numbers. Let $f_2(\sigma) : \mathbb{S}_n \mapsto \mathbb{R}^k$ be a function that is equivalent to f_1 up to input*
 241 *permutation, such that $f_2(\sigma) = f_1(\sigma'\sigma)$ for a fixed $\sigma' \in \mathbb{S}_n$. Then, the multi-orbit skew spectra of f_2*
 242 *and f_1 are equal.*

243 *Proof.* Consider a function $f_1(\sigma) : \mathbb{S}_n \mapsto \mathbb{R}^k$. Now consider a second function $f_2(\sigma) = f_1(\sigma'\sigma)$,
 244 which is equivalent to f_1 up to a permutation $\sigma' \in \mathbb{S}_n$ of its input. We can show that *each single*
 245 *entry* of the skew spectrum for f_2 is equal to the entry for f_1 , using the fact that $\rho^\dagger(g)\rho(g) = \mathbb{I}$ and
 246 that $\sum_{g \in \mathbb{G}} f(g'g) = \sum_{\hat{g} \in \mathbb{G}} f(\hat{g})$ for any group \mathbb{G} , any fixed element $g' \in \mathbb{G}$, and any function f
 247 defined over the group.

$$\begin{aligned}
 \mathcal{S}(f_2; \sigma, \rho) &= \frac{1}{(n!)^2} \sum_{\tilde{\sigma}_1 \in \mathbb{S}_n} \sum_{\tilde{\sigma}_2 \in \mathbb{S}_n} f_2(\tilde{\sigma}_1) \otimes f_2(\tilde{\sigma}_1\sigma) \otimes f_2(\tilde{\sigma}_2) \otimes (\rho(\tilde{\sigma}_1)^\dagger \rho(\tilde{\sigma}_2)) \\
 &= \frac{1}{(n!)^2} \sum_{\tilde{\sigma}_1 \in \mathbb{S}_n} \sum_{\tilde{\sigma}_2 \in \mathbb{S}_n} f_1(\sigma'\tilde{\sigma}_1) \otimes f_1(\sigma'\tilde{\sigma}_1\sigma) \otimes f_1(\sigma'\tilde{\sigma}_2) \otimes (\rho(\tilde{\sigma}_1)^\dagger \rho(\tilde{\sigma}_2)) \\
 &= \frac{1}{(n!)^2} \sum_{\hat{\sigma}_1 \in \mathbb{S}_n} \sum_{\hat{\sigma}_2 \in \mathbb{S}_n} f_1(\hat{\sigma}_1) \otimes f_1(\hat{\sigma}_1\sigma) \otimes f_1(\hat{\sigma}_2) \otimes (\rho(\sigma'^{-1}\hat{\sigma}_1)^\dagger \rho(\sigma'^{-1}\hat{\sigma}_2)) \\
 &= \frac{1}{(n!)^2} \sum_{\hat{\sigma}_1 \in \mathbb{S}_n} \sum_{\hat{\sigma}_2 \in \mathbb{S}_n} f_1(\hat{\sigma}_1) \otimes f_1(\hat{\sigma}_1\sigma) \otimes f_1(\hat{\sigma}_2) \otimes (\rho(\hat{\sigma}_1)^\dagger \rho(\sigma'^{-1})^\dagger \rho(\sigma'^{-1}) \rho(\hat{\sigma}_2)) \\
 &= \frac{1}{(n!)^2} \sum_{\hat{\sigma}_1 \in \mathbb{S}_n} \sum_{\hat{\sigma}_2 \in \mathbb{S}_n} f_1(\hat{\sigma}_1) \otimes f_1(\hat{\sigma}_1\sigma) \otimes f_1(\hat{\sigma}_2) \otimes (\rho(\hat{\sigma}_1)^\dagger \rho(\hat{\sigma}_2)) \\
 &= \mathcal{S}(f_1; \sigma, \rho)
 \end{aligned}$$

248 where we relabeled $\hat{\sigma}_1 = \sigma'\tilde{\sigma}_1$ and $\hat{\sigma}_2 = \sigma'\tilde{\sigma}_2$. □

249 The key intuition here is that the functions of two isomorphic graphs are equal up to a translation by
 250 the permutation $\bar{\sigma}$ that links their respective adjacency matrices: let $f_{\mathcal{G}}$ be the function corresponding
 251 to the original graph and let $f_{\bar{\mathcal{G}}}$ be the function given by the permuted adjacency matrix, then
 252 $f_{\bar{\mathcal{G}}}(\sigma) = f_{\mathcal{G}}(\bar{\sigma}\sigma)$. Summing over all the elements of \mathbb{S}_n neutralizes this translation.

253 C Extra experiments

254 C.1 Synthetic dataset - weighted and directed

255 We repeated the same experiment of Section 3.1, with directed, weighted, and labeled graphs. Figure 2
 256 reports the representatives of the four new families. Each edge has a weight in the interval $(0, 2]$.

257 Even in this case, the concatenation of the single orbit skew spectra allow the random forest to achieve
 258 an accuracy of 0.5, while the 2-orbit skew spectra allow for an accuracy of 1.

259 C.2 Eigenvalue collisions

260 If we consider labeled graphs, then the eigenvalues or singular values, will be a valid invariant
 261 for them. Indeed a permutation matrix would only rotate the adjacency matrix, without changing

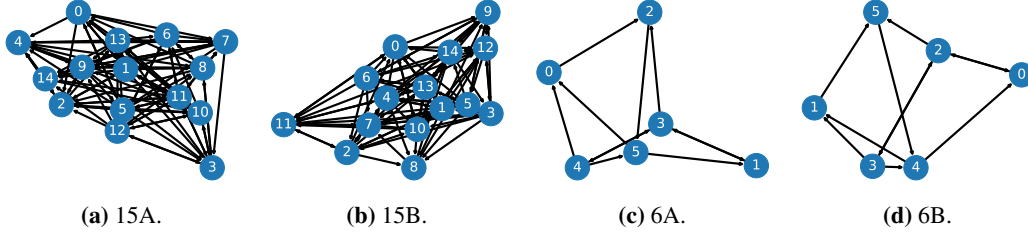


Figure 2: Synthetic dataset's graph families representatives. Graphs are directed and each edge has a weight in $(0, 2]$.

262 the eigenvalues. However, it is easy to find examples of non-isomorphic labeled graphs where the
 263 eigenvalue invariant will collide. A valid example is the given by the graphs in Fig. 3.

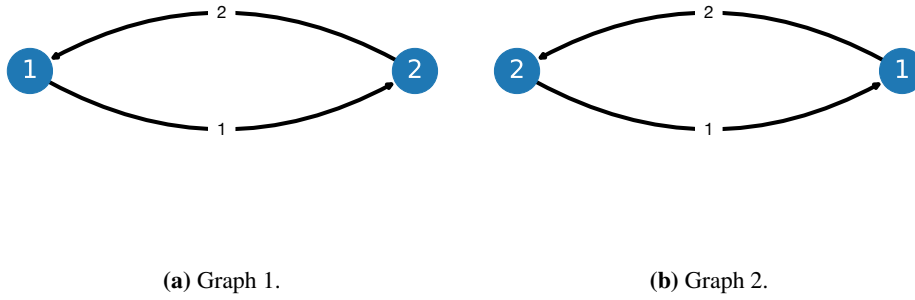


Figure 3: Example of two graphs with the same eigenvalues/singular values, but with distinct (reduced) skew spectra.

264 In the graph of Fig. 3a, we have that the node with label 1 goes to the one labeled 2 with a weight
 265 of 1. However, in the graph of Fig. 3b, the cost of moving from 1 to 2 is 2 and the two graphs are
 266 non-isomorphic. The two adjacency matrices of the graphs in Fig. 3 are

$$A_1 = \begin{bmatrix} 1 & 1 \\ 2 & 2 \end{bmatrix} \quad A_2 = \begin{bmatrix} 2 & 1 \\ 2 & 1 \end{bmatrix}. \quad (8)$$

267 It is easy to verify that $\text{Eigs}(A_1) = \{3, 0\}$ and $\text{Eigs}(A_2) = \{3, 0\}$. Similarly, $\text{SingVals}(A_1) =$
 268 $\text{SingVals}(A_2) = \{3.16227766, 0\}$. However, the reduced skew spectra of the two graphs are
 269 different, meaning that the skew spectrum manages to distinguish the two cases.